8110–8119 *Nucleic Acids Research, 2021, Vol. 49, No. 14* *Published online 13 July 2021*
https://doi.org/10.1093/nar/gkab550

The cooperative assembly of shelterin bridge provides a kinetic gateway that controls telomere length homeostasis

Jinqiang Liu[1,†], Xichan Hu[1,†], Kehan Bao[2], Jin-Kwang Kim[1], Catherine Zhang[1], Songtao Jia[2] and Feng Qiao[1,*]

[1]Department of Biological Chemistry, School of Medicine, University of California, Irvine, CA 92697-1700, USA and [2]Department of Biological Sciences, Columbia University, New York City, NY 92697-4560, USA

Received August 05, 2020; Revised June 08, 2021; Editorial Decision June 09, 2021; Accepted June 13, 2021

ABSTRACT

Shelterin is a six-protein complex that coats chromosome ends to ensure their proper protection and maintenance. Similar to the human shelterin, fission yeast shelterin is composed of telomeric double- and single-stranded DNA-binding proteins, Taz1 and Pot1, respectively, bridged by Rap1, Poz1 and Tpz1. The assembly of the proteinaceous Tpz1-Poz1-Rap1 complex occurs cooperatively and disruption of this shelterin bridge leads to unregulated telomere elongation. However, how this biophysical property of bridge assembly is integrated into shelterin function is not known. Here, utilizing synthetic bridges with a range of binding properties, we find that synthetic shelterin bridge lacking cooperativity requires a linker pair that matches the native bridge in complex lifespan but has dramatically higher affinity. We find that cooperative assembly confers kinetic properties on the shelterin bridge allowing disassembly to function as a molecular timer, regulating the duration of the telomere open state, and consequently telomere lengthening to achieve a defined species-specific length range.

INTRODUCTION

In most eukaryotes, telomeres, the natural ends of chromosomes, are essential for stable maintenance of chromosomes, and thus our genetic information (1–4). Similar to humans, the telomere structure of fission yeast, *Schizosaccharomyces pombe*, is achieved by association of shelterin components with both double-stranded (ds) and single-stranded (ss) telomeric DNA, forming a nucleoprotein complex (5,6). Fission yeast Taz1 (TRF1/2 in humans) and Pot1 (POT1 in humans) specifically bind to telomeric double-stranded (ds) and single-stranded (ss) DNA, respectively (7,8). In fission yeast, Rap1 (9,10), Poz1 and Tpz1 (5) bridge the telomeric dsDNA binder Taz1 and ssDNA binder Pot1 through their direct protein-protein interactions, forming the Taz1–Rap1–Poz1–Tpz1–Pot1 complex (Figure 1A). Telomeres are maintained at a species-specific length range, and this telomere length homeostasis is proposed to be regulated via dynamic switching of telomeres between two states: telomerase-extendible (open) and telomerase-nonextendible (closed) states (11). Genetic deletions of shelterin components such as Taz1(8), Rap1 (9,10), Poz1 (5) or mutations that disrupt the connectivity in the shelterin bridges (Rap1–Poz1–Tpz1) lead to drastically elongated telomeres due to unregulated telomerase action on telomeres (12–15).

Our previous work showed that the Tpz1-mediated complete linkage within the shelterin bridge, rather than individual components *per se*, defines the telomerase-nonextendible state (12). Moreover, Tpz1 physically interacts with both positive and negative regulators of telomere length and executes its functional roles to coordinate shelterin and telomerase in response to cell cycle signals (16–24). Through its interaction with Ccq1, Tpz1 also recruits the Clr4 methyltransferase complex CLRC to telomeres and establishes subtelomeric heterochromatin (22,25–27). Therefore, shelterin bridge has been the emerging key player in regulating telomere length homeostasis, telomeric silencing, and possibly other telomeric functions (28–31).

Shelterin complex, like other macromolecular complexes, such as ribosomes and proteasomes, needs to assemble and turn into their functional forms in a timely and precise manner in response to cellular signals. Cooperativity is a general strategy that allows multiple components to rapidly and accurately form a higher-order complex with functional conformation (32). The fission yeast shelterin bridge, Tpz1–Poz1–Rap1 complex, has recently been shown to assemble cooperatively (33,34). The assembly pathway of this three-

*To whom correspondence should be addressed. Tel: +1 949 824 0159; Email: qiao@uci.edu
†The authors wish it to be known that, in their opinion, the first two authors should be regarded as Joint First Authors.

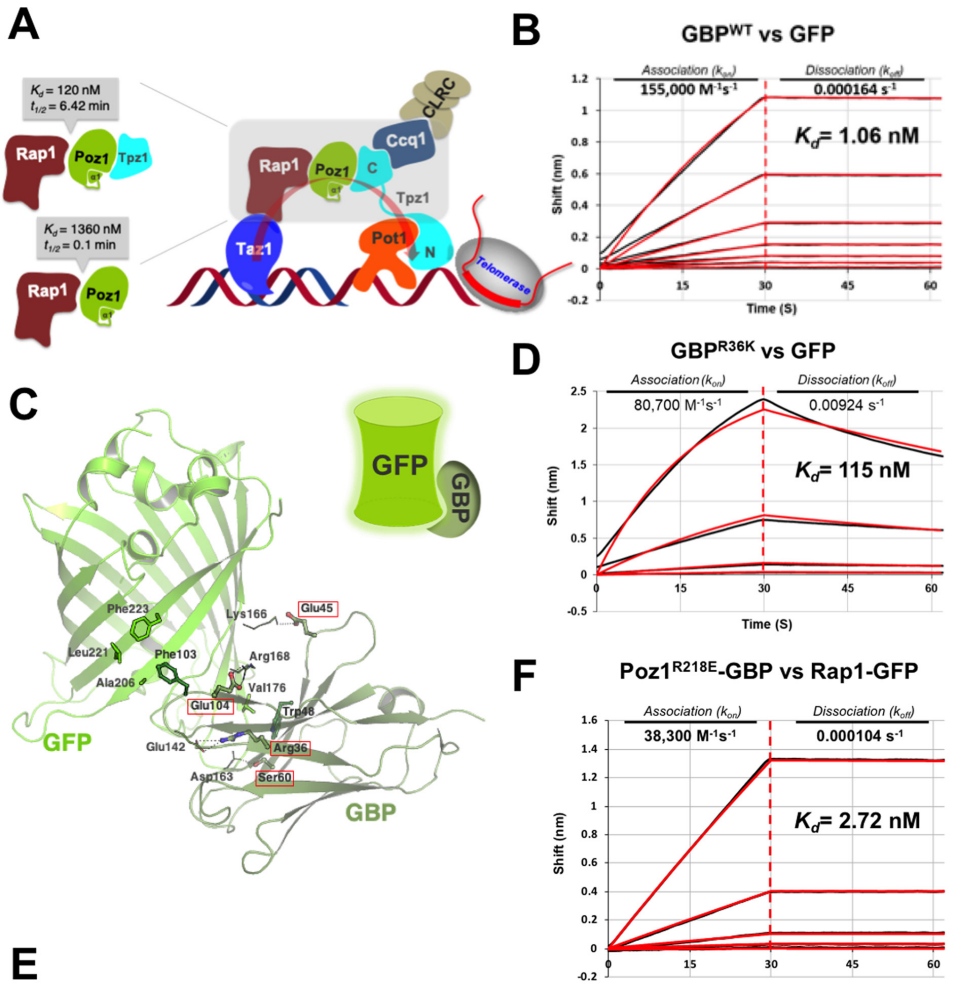

E

Name	GBP Variants	K_d	k_{off}	$t_{1/2}$
µM	E104Q	1390 nM	0.118	0.10 min
High nM	R36K/E45K	643nM	0.0442	0.26 min
Mid nM	R36K	115 nM	0.00924	1.25 min
Low nM	WT	1.06 nM	0.000164	70.4 min

Figure 1. Construction of synthetic shelterin bridges utilizing GFP-GBP pairs of variable binding properties. (**A**) Schematic diagram of *S. pombe* shelterin complex (right) and Tpz1-Poz1-Rap1 interaction (left). *Right*: Overview of *S. pombe* shelterin complex. Rap1, Poz1, and Tpz1 connect double-stranded and single-stranded telomeric DNA binding proteins, Taz1 and Pot1, respectively, forming the shelterin bridge through their protein interactions. Telomerase and histone H3K9 methyltransferase Clr4 complex (CLRC) are recruited to telomeric DNA through shelterin components. For clarity, only one copy of each component is shown, which does not represent the stoichiometry of shelterin complex in cells. *Left*: Binding affinity and half-life calculated from dissociation constant (k_{off}) of free or Tpz-bound form of Poz1 to Rap1 as reported previously. (**B**, **D** and **F**) Bio-layer interferometry (BLI) measurement of dissociation and association events in real time between GFP and GBP variants using Octet red96. A 1:1 binding model is used to fit binding curves globally, yielding equilibrium dissociation constant (K_d), association (k_{on}), and dissociation (k_{off}) rate constants. BLI experiments were repeated three times and representative results were shown. (**C**) Structure of GFP-GBP complex and the interface residues. Residues selected in this study to mutate are highlighted with red boxes. (**E**) Summary of binding properties for GFP and GBP variants interactions. Half time ($t_{1/2}$) of the protein interaction is calculated using $t_{1/2} = \ln 2/k_{off}$.

component complex was revealed at the atomic resolution (33). Tpz1–Poz1–Rap1 complex assembly is initiated by the binding of Tpz1 to Poz1, which induces the folding of the N-terminal helix in Poz1, called 'conformational trigger'. Consequently, formation of new hydrophobic interactions and hydrogen bonds within Poz1 ensues, which results in conformational changes at the Rap1-binding surface of Poz1, enhancing the binding affinity (K_d) of Poz1–Rap1 interaction 10 times and decreasing its dissociation rate (k_{off}) 60 times (Figure 1A) (33). Loss of the conformational trigger by deleting the N-terminal helix in Poz1 (Poz1ΔNTD) causes breakdown of shelterin bridges on telomeres, and leads to unregulated telomere elongation, indicating the essential role that cooperative assembly plays in telomere function. However, how this biochemical feature is integrated into shelterin function in telomere length regulation is not known.

In this study, utilizing the well-studied GFP and GFP nanobody (also called GFP Binding Protein or **GBP**) pair (35), we engineered a spectrum of GBP variants that interact with GFP with different thermodynamic and kinetic properties. We then physically tethered the GFP–GBP variant pairs to shelterin components and tested their ability to rescue shelterin bridge defective in cooperative assembly. To rescue telomere length, synthetic shelterin bridge without cooperativity requires a GFP-GBP pair with 30-fold higher binding affinity (K_d) than that of the native shelterin bridge. Interestingly, this synthetic shelterin bridge recapitulates the assembly kinetics of the native shelterin bridge, having similar dissociation rate (k_{off}) and thus half-life ($t_{1/2}$). Indeed, our previous work indicates that the assembly of shelterin bridge (Tpz1–Poz1–Rap1 complex) is promoted by the Tpz1–Poz1 interaction, which enhances Poz1–Rap1 interaction mainly by decreasing the dissociation rate of Rap1 from Tpz1-bound Poz1 (33). Therefore, cooperative assembly installs a 'kinetic gateway' in the shelterin bridge that controls timespan of the formation-and-breakage of the shelterin bridge and thus the accessible timespan for telomerase to telomeres. In contrast, telomeric silencing function of shelterin bridge is less dependent on the kinetics of its assembly, but more on its binding affinity, agreeing with its role in passively recruiting and enriching the histone H3K9 methyltransferase Clr4 to telomeres (25).

MATERIALS AND METHODS

Yeast strains, gene tagging, and mutagenesis

Fission yeast strains used in this study are listed in Supplementary Table S1. Wild-type tagging strains and single mutant strains were constructed by one-step gene replacement of the entire ORF with the C-terminus epitope-tags followed by selectable markers. The pFA6a plasmid modules were used as templates for epitope-tags and selectable markers (36). The GFP-3Flag and GBP-13myc tagging plasmids were engineered from pFA6a–GFP–KanMX6 and pFA6a–GBP–hphMX6 plasmids through mutagenesis PCR, respectively (25). Double mutant strains were produced by mating, sporulation, dissection, and selection followed by PCR verification of genotypes. All mutations were confirmed by DNA sequencing (Eton, San Diego, CA). For serial dilution plating assays, 10-fold dilutions of a log-phase culture were plated on the indicated medium and grown for 4 d at 30°C.

Protein expression and purification

Target proteins were subcloned into modified pET28a vector containing either 10His-Smt3 tag or the Avi-6His-SUMO tag (37). Plasmids were transformed into Rosetta-BL21 (DE3) cells for protein expression, which was induced with 0.4 mM IPTG for 4 h at 30°C. For biotinylated proteins, a pBirAcm vector was co-transformed. Cells were disrupted by sonication in lysis buffer (25 mM Tris–HCl at pH 8.0, 350 mM NaCl, 15 mM imidazole, 5 mM β-mercaptoethanol, 1 mM PMSF, 2 mM benzamidine). The supernatant was cleared with centrifuge and incubated with Ni-NTA (Qiagen) resin for 1 h. The elution buffer (lysis buffer plus 300 mM imidazole) was used to elute the proteins from resin. Proteins were then further purified with gel filtration columns.

Biolayer interferometry (BLI) and kinetics measurement

The BLI experiment and data analysis were performed as previously described (33). Briefly, biotinylated GBP proteins, including WT and mutants, were loaded on Streptavidin-biosensor tips, followed by quenching free streptavidin with biocytin. GFP was added to measure association and dissociation rate. Data was analyzed with ForteBio Data analysis version 9.0 and fitted with global/1:1 binding model. Equilibrium dissociation constant (K_d) and association (k_{on}) and dissociation (k_{off}) rate constants were calculated directly from software; half-life ($t_{1/2}$) was then further calculated from k_{off}.

Telomere length analysis

The telomere length of each strain was analyzed as previously described (17). Briefly, cells were successively cultured on YEAU plates and genomic DNA from each generation was prepared from 5 ml liquid culture inoculated from plates. The telomeric fragments were released by ApaI (NEB) digestion and separated on 1.8% agarose gels. Southern blots with both telomeric and *sir2*$^+$ probes were visualized using Typhoon scanner.

Co-Immunoprecipitation

As previously described (33), the indicated strains were cultured in 50 ml YEAU and harvested at log phase. Cell pellets were then washed and cryogenically disrupted with FastPrep MP with two pulses (60 sec) of bead-beating in ice-cold lysis buffer (50 mM HEPES at pH 7.5, 140 mM NaCl, 15 mM EGTA, 15 mM $MgCl_2$, 0.1% NP40, 0.5 mM Na_3VO_4, 1 mM NaF, 2 mM PMSF, 2 mM benzamidine, Complete proteinase inhibitor [Roche]). After clearing by centrifugation, protein concentrations were measured via Bradford assay and adjusted to 12 mg/ml. Anti-Flag M2 affinity gel (Sigma), anti-Myc (9E10 from Santa Cruz Biotechnology) or anti-Ccq1 rabbit serum plus IgG beads (Roche) was used for immunoprecipitation, followed by eluting with 30 μl 0.1 M glycine (pH 2.0) at room temperature for 10 min. The

elute was immediately neutralized with 2 μl 2 M Tris–HCl, pH 8.0. SDS-PAGE (8%) and western blotting using monoclonal anti-Flag (M2-F1804, from Sigma), monoclonal anti-Myc (from Covance), monoclonal anti-PK (ab27671 from Abcam), anti-Ccq1 rabbit serum (16), or anti-Cdc2 (y100.4, from Abcam) were performed to detect protein–protein interaction as indicated.

RESULTS

Design synthetic shelterin bridge with GFP–GBP pairs of variable binding properties

Recent genetic, biochemical and structural studies utilizing model organism fission yeast, *S. pombe,* have uncovered that the shelterin bridge connecting telomeric dsDNA and ssDNA controls the extendible and non-extendible states of the telomeres (12,15). In addition, the integrity of shelterin bridge is also required for telomeric heterochromatin formation (25,26). Crystal structures of fission yeast shelterin bridge (Tpz1–Poz1–Rap1 complex) have provided atomic views of the shelterin bridge and revealed cooperative assembly as the fundamental principle of shelterin bridge formation (33,34). In this process, Tpz1–Poz1 interaction induces conformational changes in Poz1, which greatly enhances the binding of Rap1 to Poz1, forming a stable shelterin bridge (33). To elucidate the biological significance of the cooperativity in the shelterin bridge assembly, we aimed to interrogate whether the allosterically enhanced thermodynamic binding affinity (K_d) or the kinetic stability (k_{off}) of the shelterin bridge originating from Tpz1-induced conformational changes of Poz1 is the key factor in regulating proper telomere length control and telomeric silencing.

To deconvolute the purpose of employing cooperative assembly mechanism for shelterin bridge assembly, we constructed synthetic shelterin bridges utilizing protein-protein interaction module GFP-GBP with variable binding properties. The GFP Binding Protein (GBP) is a GFP nanobody, a single-chain V_HH antibody domain developed to bind to GFP with high specificity (35). The wild-type GBP interacts with GFP with a thermodynamic dissociation constant (K_d) of 1.06 nM, which is over 113 times stronger than the binding of Rap1 to Tpz1-bound Poz1. Moreover, the GFP–GBP complex also has very slow dissociation rate with $k_{off} = 1.64 \times 10^{-4}$ s^{-1}, thus the half-life (the time in which half of the initially present complexes have dissociated—1n $2/k_{off}$) being 70.4 min, about 10 times longer than that of the Tpz1-bound Poz1–Rap1 complex (6.42 min) and 700 times longer than that of the free Poz1–Rap1 (0.1 min) (Figure 1B). To construct synthetic shelterin bridges with a wide spectrum of thermodynamic and kinetic properties, we set out to design a series of GBP mutants that have decreased interaction affinity with GFP based on the crystal structure of GFP-GBP heterodimer complex. GBP-GFP interaction is mostly driven by hydrophobic interactions between F102 and L221, A206 of GBP and F223 of GFP, as well as between W47 of GBP and V176 of GFP. Around the hydrophobic core, GBP forms salt bridges with GFP via its R36, E45 and E104 to enhance specificity and affinity (Supplementary Figure S1A). To weaken, rather than disrupt GFP-GBP interaction, we selected residues around the edge, but not in the hydrophobic core of the GFP-GBP interface (highlighted residues in Supplementary Figure S1A). Thus, we introduced mild changes to GBP by mutating these residues to amino acids with similar properties (Figure 1C). We aimed to select for GBP mutants that have a range of binding affinities with GFP (to be named low nM, middle nM, high nM, and μM) and carried out binding assays using Bio-layer interferometry (BLI) to measure both the thermodynamic binding affinity (K_d) and kinetic behavior (k_{off}) of the GFP-GBP variant pairs. As shown in Figure 1B, D, and Supplementary Figure S1B, we successfully achieved this goal by obtaining GFP-interacting GBP variants— GBP^{R36K} (115 nM: mid nM), $GBP^{R36K/E45K}$ (643 nM: high nM) and GBP^{E104Q} (1.39 μM: μM). Together with GBP^{WT} (1.06 nM: low nM), we have GFP-GBP pairs with their binding affinities (K_d) ranging from 115 nM to 1.39 μM levels, and dissociation constant (k_{off}) ranging from 0.00016 to 0.12 s^{-1} (correspondingly, the converted half-life $t_{1/2}$ from 70.4 min to 0.1 min). Among them, GBP^{R36K} binds to GFP with a similar affinity as Tpz1-bound Poz1–Rap1 (115 nM versus 120 nM), but shorter half-life (1.25 min versus 6.42 min). GBP^{E104Q} binds to GFP with a similar affinity and half-life to Poz1–Rap1 interaction (1390 nM versus 1360 nM). $GBP^{R36K/E45K}$ lies between the above two GBP variants. GBP^{WT} can provide extremely high affinity and long half-life (70.4 min). With this set of GBP variant-GFP pairs (Figure 1E), we were able to engineer shelterin bridge with synthetic bridges of a wide range of binding properties to investigate which biochemical properties of shelterin bridge enabled by cooperative assembly are determinants of telomere length regulation.

Slower dissociation rate rather than increased binding affinity is the key contribution of cooperative shelterin bridge assembly to telomere length regulation

The cooperative interaction between Rap1 and Poz1 induced by Poz1–Tpz1 interaction has been elucidated at atomic level in our previous study (33), in which Poz1-R218E was identified as a mutant defective in Poz1–Rap1 interaction. This mutation disrupts a major salt bridge between Poz1–R218 and Rap1–E476. Moreover, deletion of the extended Poz1-interaction domain of Rap1 (Rap1ΔPID) also results in defective Poz1–Rap1 interaction. Importantly, both Poz1-R218E and Rap1ΔPID mutants selectively disrupt the Poz1–Rap1 interaction without affecting other interactions within the shelterin bridge. Furthermore, when GBP^{WT} and GFP were fused with $Poz1^{R218E}$ and Rap1, respectively, $Poz1^{R218E}$–GBP interacts with Rap1-GFP with similar affinity as GBP–GFP (Figure 1F). Therefore, in either *poz1-R218E* or *rap1ΔPID* background, physically linking Poz1 and Rap1 using identified GBP–GFP pairs with a range of thermodynamic and kinetic properties would provide a route to investigate the significance of the cooperative assembly that exists in Tpz1-induced Poz1-Rap1 interaction.

We first assessed the consequence of using GFP–GBP variants to rescue telomere elongation in *poz1-R218E* background due to the disruption of Poz1–Rap1 interaction

within the shelterin bridge. In these strains, *poz1*$^+$ was tagged with GBP variants, and *rap1*$^+$ was tagged with GFP (Figure 2A). As expected, *poz1-R218E* strain itself causes telomere massive elongation to ∼3 kb due to loss of negative regulation from the connected shelterin bridge. However, telomeres in *poz1-R218E* background with GFP-GBP variants linking *poz1-R218E* and *rap1*$^+$ showed various degrees of decreased length compared to the ∼3 kb telomeres in *poz1-R218E* cells (Figure 2B). Accordingly, the interactions among shelterin components were also rescued in a quantitative fashion as shown by co-immunoprecipitation experiments (Figure 2C and D). Evidently, the rescued interactions are independent of telomeric DNA as the tested interactions are equally strong in DNase-treated controls (Figure 2D and Supplementary Figure S2C). As expected, the tighter the binding between GFP and GBP, the shorter the telomere length (Figure 2B). Interestingly, low nM GFP-GBP pair can rescue the telomere length to the wild-type level, whereas mid nM GFP-GBP pair still have telomeres about 200 bp longer than the wild-type strain. The same outcome was also recapitulated in the GFP–GBP pair-linked Rap1-Poz1 in the *rap1ΔPID* or *poz1-R218E/rap1ΔPID* double mutant background (Supplementary Figure S2A and S2B), indicating that telomere length restoration is due to GFP–GBP pair-mediated linkage and is independent of the way that shelterin bridge is disrupted. In addition, in *poz1-R218E* background, when GFP–GBP pair tethers *tpz1*$^+$ and *poz1-R218E*, telomere length was not restored, indicating the telomere length restoration is not due to GFP-GBP pair itself (Supplementary Figure S2D); instead, it is due to the rescued Poz1-Rap1 interaction via GFP-GBP pair. It is worth noting that the native interface between Rap1 and Poz1-Tpz1 in the shelterin bridge has binding affinity close to Mid nM GFP-GBP pair (120 nM vs. 115 nM). However, our experiments indicate that similar affinity by itself cannot fully rescue the telomere length regulation defect. Instead, to fully rescue telomere length, synthetic shelterin bridge without cooperativity requires a GFP-GBP pair with ∼110-fold higher binding affinity ($K_d^{GFP–GBP}$ = 1.06 nM versus native shelterin bridge = 120 nM) than that of the native shelterin bridge. This suggests that other advantages provided by cooperative shelterin bridge assembly, rather than thermodynamic affinity, play determining roles in telomere length regulation.

We then compared binding kinetics of the synthetic shelterin bridges (GFP-GBP pairs) with that of Rap1 and Poz1–Tpz1 interaction studied extensively before (33). Based on its k_{off}, and thus half-life ($t_{1/2} = \ln 2/k_{off}$), Poz1 and Rap1 interaction is intrinsically unstable with half of the complexes disassembling every 0.1 min. Tpz1 stabilizes the Poz1–Rap1 interaction with an increased half-life of 6.42 min, over 60-fold increase. Among the four GFP–GBP pairs, only the Low nM GFP–GBP^{WT} pair offers longer half-life than the native shelterin bridge (70.4 min versus 6.42 min). For Mid nM GFP–GBP^{R36K} pair, although its K_d is similar to that of the native shelterin bridge, its half-life (1.25 min) is about 5-fold shorter. The failure of Mid nM GFP–GBP^{R36K} pair to restore telomere length implies that binding kinetics (k_{off} or $t_{1/2}$), rather than binding strength (K_d), could contribute more to telomere length regulation.

To further explore the contribution of shelterin bridge lifespan to telomere length regulation, we screened and obtained two more GFP-GBP variant pairs, which have a more similar half-life $t_{1/2}$ to the native shelterin bridge, GFP-GBP^{E45K} ($t_{1/2}$ = 15.16 min) and GFP-GBP^{S60G} ($t_{1/2}$ = 18.02 min), and 30-fold higher affinity (Supplementary Figure S1B). Indeed, when we introduced these two pairs of synthetic shelterin bridges to *poz1-R218E* strain background as before, we found that both of them can almost fully restore the telomere length (Figure 2F), certainly to a comparable level to GFP-GBP^{WT}. Thus, the kinetic lifespan of shelterin bridge assembly, rather than its thermodynamic affinity, plays a determining role in telomere length control. The extensively elongated lifespan of the shelterin bridge complex stemming from the Tpz1-Poz1-Rap1 cooperative assembly might control the timespan of telomerase to telomere ends to regulate telomerase action. Therefore, cooperative assembly provides a 'kinetic gateway' in shelterin bridge that controls the timespan of 'open' and 'closed' states of telomeres. Shorter half-life of shelterin bridge (such as those in Mid nM, High nM and μM synthetic shelterin bridges) leads to longer 'open state' of the telomeres, thus providing more opportunities for telomerase to elongate telomeres.

Rescuing of telomeric silencing only depends on the binding affinity within synthetic shelterin bridge

The complete linkage among shelterin components (Taz1–Rap1–Poz1–Tpz1–Ccq1) (Figure 3A) is required to recruit CLRC to telomeric region for subtelomeric heterochromatin assembly, thus telomere silencing effect (25). To evaluate the function of cooperativity in shelterin-mediated heterochromatin assembly, we assessed silencing of *ura4*$^+$ reporter gene located adjacent to telomere region on a minichromosome. Consistent with previous studies (38), silencing of *TEL::ura4*$^+$ is defective in *rap1ΔPID* cells due to the comprised shelterin bridge, resulting in cell lethality on +FOA plates. As expected, the defective silencing of *TEL::ura4*$^+$ is gradually alleviated in the strains with synthetic shelterin bridges. More cells are able to grow on +FOA plate along with stronger GFP-GBP variants interaction (Figure 3B). Indeed, co-IP results also confirmed the restoration of the recruitment of CLRC by the shelterin complex, which was indicated by the rescued interaction between Rap1 and Clr4 with Mid nM GFP–GBP^{R36K} and Low nM GFP–GBP^{WT} synthetic shelterin bridges (Figure 3C). Unexpectedly, although Low nM GFP-GBP^{WT} restored Rap1-Clr4 interaction much more than the Mid nM GFP-GBP^{R36K} did (over 20-fold, correlated with their K_d), both of them can restore the telomeric silencing effect to a similar level (Figure 3B). Therefore, differing from telomere length regulation that requires slower dissociation kinetics enabled by the cooperative assembly, restoration of shelterin bridge to the wild-type binding affinity (Mid nM) is sufficient to rescue telomeric silencing. This result agrees with the passive recruitment role of shelterin in enriching CLRC methyltransferase complex onto the subtelomere regions for gene silencing, a process independent of time scale (25).

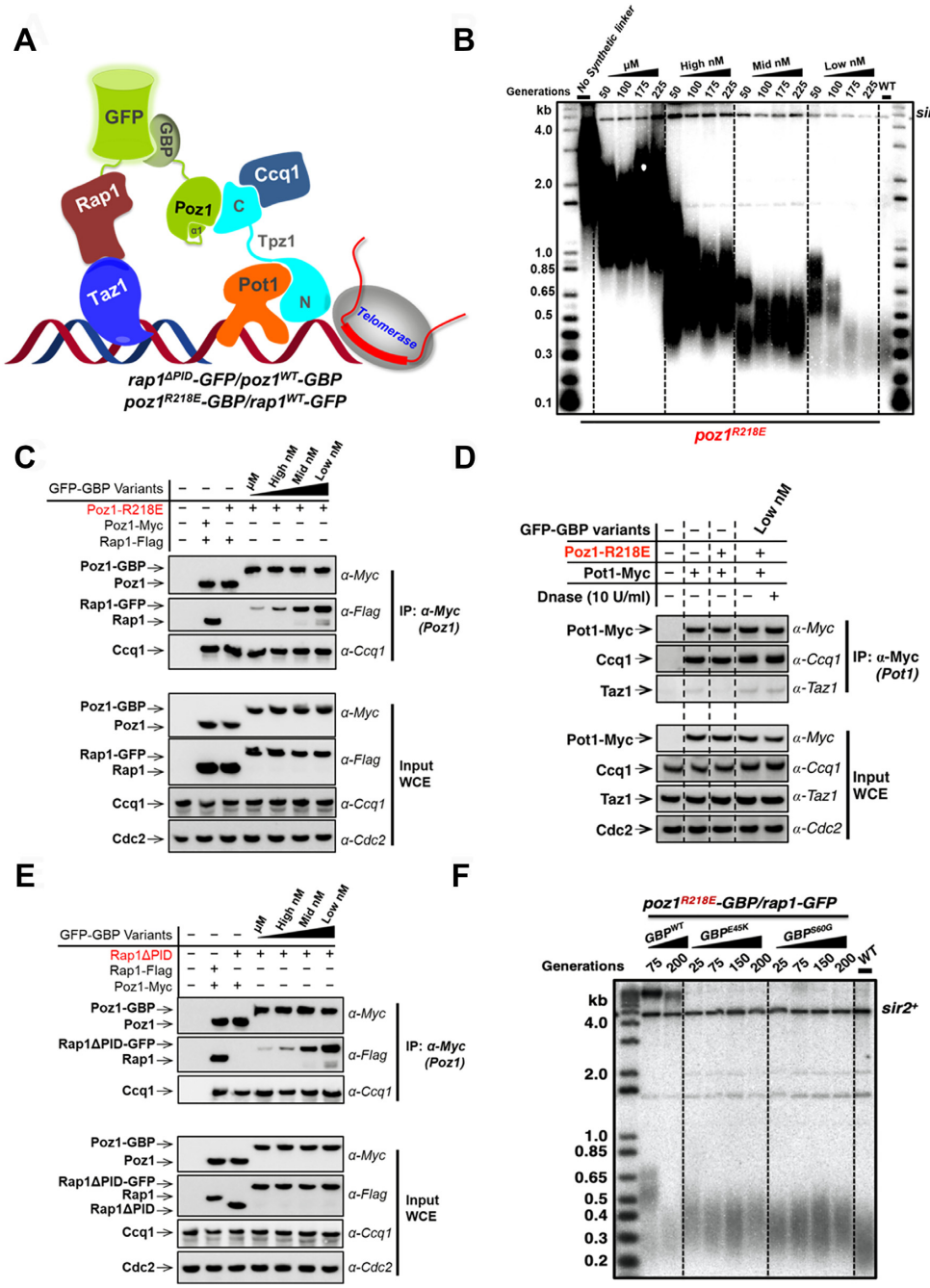

Figure 2. Slower dissociation rate rather than increased binding affinity is the key contribution of cooperative shelterin bridge assembly to telomere length regulation. (**A**) Schematic diagram of the synthetic *S. pombe* shelterin bridge with disrupted Rap1-Poz1 interaction. GFP is tagged to Rap1, and GBP variants are tagged to Poz1. (**B**) Telomere length analysis of indicated synthetic shelterin bridge strains in $poz1^{R218E}$ background from successive re-streaks on agar plates via southern blotting. The telomere fragment is released from genomic DNA by ApaI digestion. Wild-type cells are denoted as WT. The mutant $poz1^{R218E}$ without synthetic shelterin bridge serve as controls and are denoted, 'No Synthetic Linker'. $sir2^{+}$ indicates an ApaI digested $sir2^{+}$ gene fragment as the loading control. In this paper, the 1 kb plus marker from Life Technologies is used in all telomere length analysis. (**C** and **E**) Co-immunoprecipitation assays evaluating interactions among shelterin components with synthetic shelterin bridges in $poz1^{R218E}$ (C) or $rap1^{\Delta PID}$ (E) background. Both Poz1-Rap1 and Poz1-Tpz1-Ccq1 interactions are measured. Cdc2 was shown as the loading control. Input: 1/30 of input WCE (whole-cell extract). (**D**) Co-immunoprecipitation assays evaluating interactions between Pot1 and Taz1 with synthetic shelterin bridges in $poz1^{R218E}$ background. DNase was used to evaluate whether the binding is dependent or independent of telomere DNA. Pot1-Ccq1 interaction was also measured as positive control. Cdc2 was shown as the loading control. Input: 1/30 of input WCE (whole-cell extract). (**F**) Telomere length analysis of $poz1^{R218E}$ strains with GFP-GBP^{E45K} and GFP-GBP^{S60G} pairs as synthetic shelterin bridges, which have similar half-life as the native shelterin bridge.

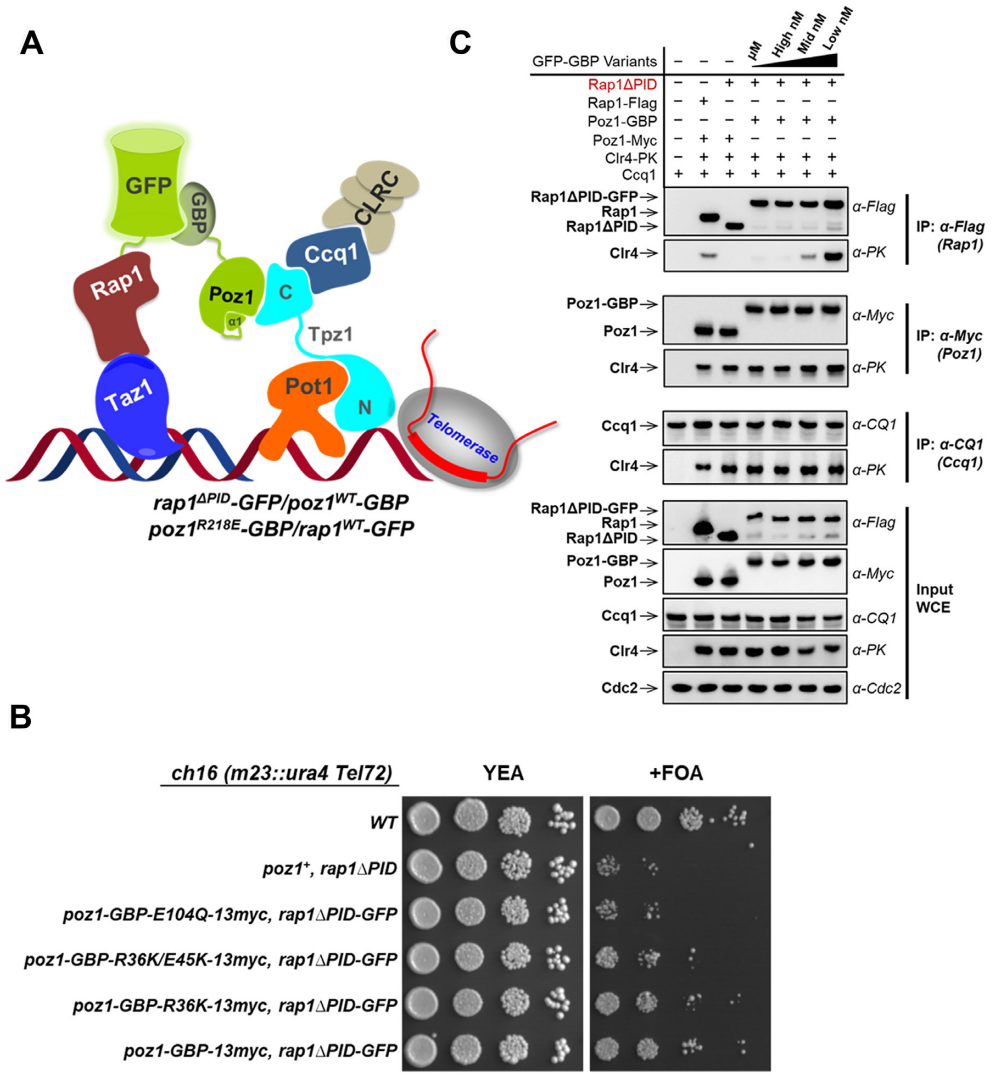

Figure 3. Shelterin-mediated telomeric silencing depends on the binding affinity within synthetic shelterin bridge. (**A**) Schematic diagram of the synthetic shelterin bridge recruiting CLRC complex to the telomere in *rap1*$^{\Delta PID}$ background. (**B**) Tenfold serial dilution analyses of synthetic shelterin strains with *rap1*$^{\Delta PID}$ grown on the indicated media to measure the expression of *TEL::ura4+*. (**C**) Co-immunoprecipitation assays evaluating synthetic shelterin bridge in CLRC complex recruitment for corresponding strains with *rap1*$^{\Delta PID}$ background. Rap1–Clr4, Ccq1–Clr4 and Poz1–Clr4 interactions are measured.

Conformational trigger in Poz1 is the key element for the 'kinetic gateway'

In the process of cooperative shelterin bridge assembly, the very N-terminus of Poz1 (Poz1-NTD) has been shown to trigger the conformational changes in Poz1 upon Poz1–Tpz1 interaction (33). The conformational changes in Poz1 enhance Poz1–Rap1 interaction by increasing Poz1-Rap1 binding affinity and decreasing dissociation rate. Deletion of Poz1-NTD (Poz1ΔNTD) completely abolishes the high binding affinity binding between Poz1 and Rap1 even in the presence of Tpz1. As a result, *poz1ΔNTD* cells have drastically elongated telomeres. Interestingly, in *poz1ΔNTD* cells, Poz1-Rap1 interaction is disrupted and Poz1–Tpz1–Ccq1 interaction is diminished (33), indicating the essential role of the 'conformational trigger' in regulating shelterin bridge and thus controlling telomere length. Therefore, we aimed to assess whether the 'conformational trigger' controls the 'kinetic gateway'. Taking advantage of our GFP-GBP variant pairs, we fused the Low nM pair to Poz1–Rap1 and Poz1–Tpz1, respectively. Then, we assessed the shelterin bridge assembly in both settings via co-IP experiments. In the *poz1ΔNTD-GBP*^{WT}*/rap1-GFP* strain (Figure 4A), we clearly observed that both Poz1-Rap1 interaction (Figure 4B) and the telomere length (Figure 4C) were restored to the wild-type level. Intriguingly, Poz1–Tpz1–Ccq1 interaction was also partially restored (Figure 4B). On the other hand, in the *poz1ΔNTD-GBP*^{WT}*/tpz1-GFP* background (Figure 4D), Poz1–Tpz1–Ccq1 interaction was fully rescued, but the synthetic linker had little effect on Poz1–Rap1 interaction (Figure 4E). These results suggest that Poz1-NTD, the 'conformational trigger', rather than Poz1–Tpz1 interaction per se, plays an essential role in shelterin bridge assembly by controlling Poz1–Rap1 interaction kinetics, which influences the Poz1–Tpz1–Ccq1 interaction of the bridge. Without the 'conformational trigger', even

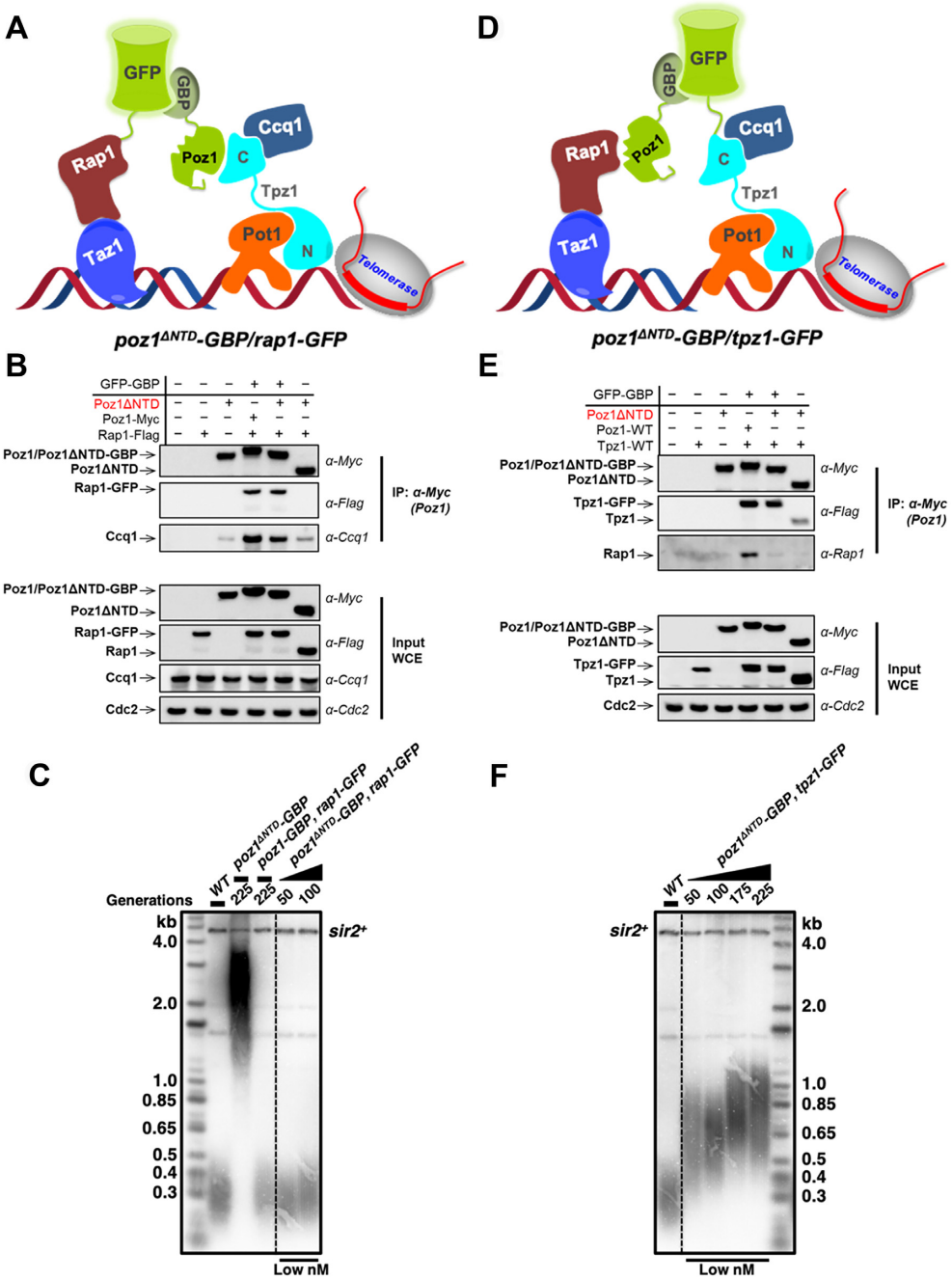

Figure 4. Conformational trigger in Poz1 is the key element for the 'kinetic gateway'. (**A** and **D**) Schematic diagram of the synthetic *S. pombe* shelterin complex with conformational trigger in Poz1 deleted. Rap1 (A) or Tpz1 (C) is tagged with GFP, and Poz1 is tagged with GBP^{WT}. (**B** and **E**) Co-immunoprecipitation assays evaluating the assembly of synthetic shelterin for the corresponding strains with $poz1^{\Delta NTD}$. Either Rap1–Poz1 (B) or Poz1–Tpz1 (D) is tethered via GFP-GBP pair. (**C** and **F**) Telomere length analysis of indicated synthetic shelterin strain in $poz1^{\Delta NTD}$ background. Either Rap1–Poz1 (E) or Poz1–Tpz1 (F) is tethered via GFP–GBP pair.

if Poz1 and Tpz1 are connected, Poz1 still cannot interact with Rap1. Agreeing with the co-IP results, whereas Low nM synthetic bridge in the *poz1ΔNTD-GBP^{WT}/rap1-GFP* strain can almost rescue its telomere length to the wild-type level (Figure 4C), the synthetic bridge of the same strength in *poz1ΔNTD-GBP^{WT}/tpz1-GFP* strain failed to restore the telomere length to the same level (Figure 4F). Not surprisingly, synthetic bridge of lower strength, such as Mid nM and μM GFP–GBP pairs, cannot restore the telomere length to the wild-type level either (Supplementary Figure S3).

DISCUSSION

As Richard Feynman said, 'What I cannot create, I do not understand'. Inspired by this quote, we engineered *S. pombe*

cells with synthetic shelterin bridges to investigate the key biophysical properties in the shelterin bridge that contribute to its telomere length regulation and telomeric silencing functions. This was enabled by the creation of GFP-GBP variant pairs with a wide range of thermodynamic and kinetic properties. Utilizing these synthetic shelterin bridges, we found that kinetic properties of the shelterin assembly, such as dissociation rate (half-life), have an unrecognized contribution to telomere length regulation. The intrinsic kinetic behavior of the shelterin assembly revealed in our study indicates its importance in collaborating with telomerase to elongate telomeres. Telomere lengthening is coupled to cell cycle-regulated events at telomere regions. In late S phase, when the DNA replication machinery completes most of the genome, $Rad3^{ATR}/Tel1^{ATM}$ are activated and phosphorylate the critical Thr93 residue in Ccq1 at telomeres, priming the telomere for telomerase recruitment (19,20,39). Then, telomerase holoenzyme, is recruited via two-pronged telomere-telomerase interfaces to the telomere by the cell cycle-regulated, phospho-Thr93-mediated Ccq1–Est1 and Trt1–$Tpz1^{TEL\text{-}Patch}$ interactions (16,23). This intermediate telomerase recruitment complex further engages the telomerase core enzyme (Trt1-TER1) at the very 3′ end of the telomere for nucleotide additions. On the other hand, the substrate—telomeric DNA is also regulated. For elongation by telomerase, the very 3′ end of the telomere has to be in the extendible state. We found previously that the complete linkage between telomeric dsDNA binder and ssDNA binder controls telomeres in the non-extendible state (12). Permanent breakage of the linkage leads to drastically elongated telomeres. In this study, we demonstrated the correlation between the life span of shelterin bridge and telomere length. If the life span of the bridge is too short, for example with $t_{1/2}$ less than 2 min (in the cases of Mid nM to μM synthetic bridges, and $poz1^{\Delta NTD}$), the bridge would be mostly in the open state during the late S phase (20–40 min), thus providing telomerase a high percentage of extendible telomeres to elongate. This loss of 'open' and 'close' state control on the telomere (substrate) side leads to massive elongation of telomeres. In contrast, for native shelterin bridge assembled with cooperativity, the life span of the bridge $t_{1/2}$ is 6.42 min (Figure 5), which provides an optimal percentage of open telomeres for telomerase to elongate during the late S phase. On top of cell cycle-regulated telomerase recruitment, our study adds an additional layer of temporal regulation of telomere elongation through the kinetics embedded in shelterin complex assembly.

Interestingly, for the role of shelterin bridge in establishing heterochromatin and telomeric silencing, 10-fold difference in interaction affinity (comparing Mid nM and Low nM synthetic bridges) show almost no difference in restoring the telomeric silencing effect. This is different from telomere length regulation that requires slower dissociation kinetics enabled by the cooperative assembly. This is most likely due to the passive recruitment role of shelterin in enriching CLRC methyltransferase complex onto the subtelomere regions for gene silencing, a process independent of time scale but determined by the critical concentration of CLRC enriched by the shelterin bridge to the telomeric and subtelomeric regions. Clearly, the distinctive kinetic and thermodynamic properties of shelterin bridge contribute accordingly to the biological processes it participates in.

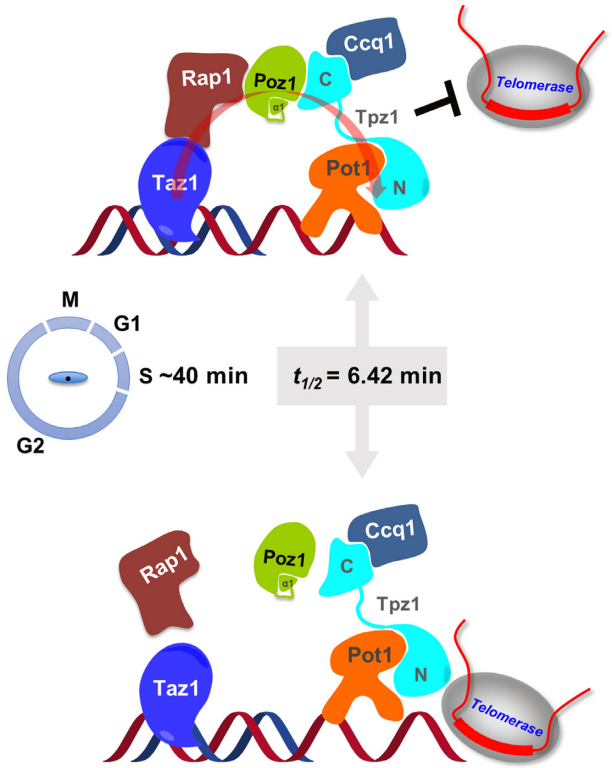

Figure 5. Model of how kinetics of shelterin bridge assembly and disassembly controls telomere elongation. Spatiotemporal regulation of telomerase-mediated telomere elongation is coupled to telomere states controlled by shelterin complex. Cooperative assembly confers kinetic properties on the shelterin bridge allowing disassembly to function as a molecular timer, regulating the switching of the telomere open and closed states to achieve a defined species-specific length range.

DATA AVAILABILITY

All data included in this study is available upon reasonable request by contacting the corresponding author.

SUPPLEMENTARY DATA

Supplementary Data are available at NAR Online.

ACKNOWLEDGEMENTS

We thank Fuyuki Ishikawa, Toru Nakamura, Julie Cooper, Virginia Zakian, Pingwei Li and Takashi Toda for providing strains, Julie Cooper for gifting Taz1 antibody, Craig Kaplan and Peter Kaiser for comments on the manuscript and helpful discussions.

Author Contributions: F.Q. conceived, designed, and supervised the study; J.L. and X.H. made various constructs, purified the proteins, and performed biochemical experiments. J.L., X.H. and J.K. analyzed the biochemical data, and J.K. made protein structure figures. J.L., X.H. and C.Z. performed genetic experiments and analyzed the data. K.B.

and S.J. performed telomeric silencing assays. J.L., J.K., K.B. and X.H. prepared the figures. F.Q. and J.L. wrote the manuscript with input from J.K., X.H., C.Z., K.B. and S.J.

FUNDING

NIH [R01GM098943]; American Cancer Society Research Scholar Grant [RSG-16–041-01-DMC to F.Q., R35GM126910 to S.J.]. Funding for open access charge: NIH.
Conflict of interest statement. None declared.

REFERENCES

1. De Lange,T. (2018) Shelterin-mediated telomere protection. *Annu. Rev. Genet.*, **52**, 223–247.
2. Wu,R.A., Upton,H.E., Vogan,J.M. and Collins,K. (2017) Telomerase mechanism of telomere synthesis. *Annu. Rev. Biochem.*, **86**, 439–460.
3. Tomita,K. (2018) How long does telomerase extend telomeres? regulation of telomerase release and telomere length homeostasis. *Curr. Genet.*, **64**, 1177–1181.
4. Nandakumar,J. and Cech,T.R. (2013) Finding the end: recruitment of telomerase to telomeres. *Nat. Rev. Mol. Cell Biol.*, **14**, 69–82.
5. Miyoshi,T., Kanoh,J., Saito,M. and Ishikawa,F. (2008) Fission yeast Pot1-Tpp1 protects telomeres and regulates telomere length. *Science*, **320**, 1341–1344.
6. Jain,D. and Cooper,J.P. (2010) Telomeric strategies: means to an end. *Annu. Rev. Genet.*, **44**, 243–269.
7. Baumann,P. and Cech,T.R. (2001) Pot1, the putative telomere end-binding protein in fission yeast and humans. *Science*, **292**, 1171–1175.
8. Cooper,J.P., Nimmo,E.R., Allshire,R.C. and Cech,T.R. (1997) Regulation of telomere length and function by a Myb-Domain protein in fission yeast. *Nature*, **385**, 744–747.
9. Kanoh,J. and Ishikawa,F. (2001) Sprap1 and Sprif1, recruited to telomeres by Taz1, are essential for telomere function in fission yeast. *Curr. Biol.*, **11**, 1624–1630.
10. Chikashige,Y. and Hiraoka,Y. (2001) Telomere binding of the Rap1 protein is required for meiosis in fission yeast. *Curr. Biol.*, **11**, 1618–1623.
11. Teixeira,M.T., Arneric,M., Sperisen,P. and Lingner,J. (2004) Telomere length homeostasis is achieved via a switch between telomerase- extendible and -nonextendible states. *Cell*, **117**, 323–335.
12. Jun,H.I., Liu,J., Jeong,H., Kim,J.K. and Qiao,F. (2013) Tpz1 controls a telomerase-nonextendible telomeric state and coordinates switching to an extendible state via Ccq1. *Genes Dev.*, **27**, 1917–1931.
13. Chen,Y., Rai,R., Zhou,Z.R., Kanoh,J., Ribeyre,C., Yang,Y., Zheng,H., Damay,P., Wang,F., Tsujii,H. *et al.* (2011) A conserved motif within RAP1 has diversified roles in telomere protection and regulation in different organisms. *Nat. Struct. Mol. Biol.*, **18**, 213–221.
14. Harland,J.L., Chang,Y.T., Moser,B.A. and Nakamura,T.M. (2014) Tpz1-Ccq1 and Tpz1-Poz1 interactions within fission yeast shelterin modulate Ccq1 Thr93 phosphorylation and telomerase recruitment. *PLos Genet.*, **10**, e1004708.
15. Pan,L., Hildebrand,K., Stutz,C., Thoma,N. and Baumann,P. (2015) Minishelterins separate telomere length regulation and end protection in fission yeast. *Genes Dev.*, **29**, 1164–1174.
16. Hu,X., Liu,J., Jun,H.I., Kim,J.K. and Qiao,F. (2016) Multi-Step coordination of telomerase recruitment in fission yeast through two coupled telomere-telomerase interfaces. *Elife*, **5**, e15470.
17. Liu,J., Yu,C., Hu,X., Kim,J.K., Bierma,J.C., Jun,H.I., Rychnovsky,S.D., Huang,L. and Qiao,F. (2015) Dissecting fission yeast shelterin interactions via micro-ms links disruption of shelterin bridge to tumorigenesis. *Cell Rep.*, **12**, 2169–2180.
18. Mennie,A.K., Moser,B.A., Hoyle,A., Low,R.S., Tanaka,K. and Nakamura,T.M. (2019) Tpz1(TPP1) prevents telomerase activation and protects telomeres by modulating the Stn1-Ten1 complex in fission yeast. *Commun Biol*, **2**, 297.
19. Chang,Y.T., Moser,B.A. and Nakamura,T.M. (2013) Fission yeast shelterin regulates DNA polymerases and Rad3(ATR) kinase to limit telomere extension. *PLoS Genet.*, **9**, e1003936.
20. Moser,B.A., Chang,Y.T., Kosti,J. and Nakamura,T.M. (2011) Tel1ATM and Rad3ATR kinases promote Ccq1-Est1 interaction to maintain telomeres in fission yeast. *Nat. Struct. Mol. Biol.*, **18**, 1408–1413.
21. Moser,B.A., Subramanian,L., Khair,L., Chang,Y.T. and Nakamura,T.M. (2009) Fission yeast Tel1(ATM) and Rad3(ATR) promote telomere protection and telomerase recruitment. *PLoS Genet.*, **5**, e1000622.
22. Armstrong,C.A., Moiseeva,V., Collopy,L.C., Pearson,S.R., Ullah,T.R., Xi,S.T., Martin,J., Subramaniam,S., Marelli,S., Amelina,H. *et al.* (2018) Fission yeast Ccq1 is a modulator of telomerase activity. *Nucleic Acids Res.*, **46**, 704–716.
23. Armstrong,C.A., Pearson,S.R., Amelina,H., Moiseeva,V. and Tomita,K. (2014) Telomerase activation after recruitment in fission yeast. *Curr. Biol.*, **24**, 2006–2011.
24. Tomita,K. and Cooper,J.P. (2008) Fission yeast Ccq1 is telomerase recruiter and local checkpoint controller. *Genes Dev.*, **22**, 3461–3474.
25. Wang,J., Cohen,A.L., Letian,A., Tadeo,X., Moresco,J.J., Liu,J., Yates,J.R. 3rd, Qiao,F. and Jia,S. (2016) The proper connection between shelterin components is required for telomeric heterochromatin assembly. *Genes Dev.*, **30**, 827–839.
26. Van Emden,T.S., Forn,M., Forne,I., Sarkadi,Z., Capella,M., Martin Caballero,L., Fischer-Burkart,S., Bronner,C., Simonetta,M., Toczyski,D. *et al.* (2019) Shelterin and subtelomeric DNA sequences control nucleosome maintenance and genome stability. *EMBO Rep.*, **20**, e47181.
27. Zofall,M., Smith,D.R., Mizuguchi,T., Dhakshnamoorthy,J. and Grewal,S.I.S. (2016) Taz1-Shelterin promotes facultative heterochromatin assembly at chromosome-internal sites containing late replication origins. *Mol. Cell*, **62**, 862–874.
28. Begnis,M., Apte,M.S., Masuda,H., Jain,D., Wheeler,D.L. and Cooper,J.P. (2018) Rnai drives nonreciprocal translocations at eroding chromosome ends to establish telomere-free linear chromosomes. *Genes Dev.*, **32**, 537–554.
29. Fernandez-Alvarez,A., Bez,C., O'Toole,E.T., Morphew,M. and Cooper,J.P. (2016) Mitotic nuclear envelope breakdown and spindle nucleation are controlled by interphase contacts between centromeres and the nuclear envelope. *Dev. Cell*, **39**, 544–559.
30. Dehe,P.M., Rog,O., Ferreira,M.G., Greenwood,J. and Cooper,J.P. (2012) Taz1 enforces cell-cycle regulation of telomere synthesis. *Mol. Cell*, **46**, 797–808.
31. Pitt,C.W. and Cooper,J.P. (2010) Pot1 inactivation leads to rampant telomere resection and loss in one cell cycle. *Nucleic Acids Res.*, **38**, 6968–6975.
32. Williamson,J.R. (2008) Cooperativity in macromolecular assembly. *Nat. Chem. Biol.*, **4**, 458–465.
33. Kim,J.K., Liu,J., Hu,X., Yu,C., Roskamp,K., Sankaran,B., Huang,L., Komives,E.A. and Qiao,F. (2017) Structural basis for shelterin bridge assembly. *Mol. Cell*, **68**, 698–714.
34. Xue,J., Chen,H., Wu,J., Takeuchi,M., Inoue,H., Liu,Y., Sun,H., Chen,Y., Kanoh,J. and Lei,M. (2017) Structure of the fission yeast *S. pombe* telomeric Tpz1-Poz1-Rap1 complex. *Cell Res.*, **27**, 1503–1520.
35. Kubala,M.H., Kovtun,O., Alexandrov,K. and Collins,B.M. (2010) Structural and thermodynamic analysis of the GFP:GFP-nanobody complex. *Protein Sci.*, **19**, 2389–2401.
36. Sato,M., Dhut,S. and Toda,T. (2005) New drug-resistant cassettes for gene disruption and epitope tagging in *Schizosaccharomyces pombe*. *Yeast*, **22**, 583–591.
37. Zhao,B., Shu,C., Gao,X., Sankaran,B., Du,F., Shelton,C.L., Herr,A.B., Ji,J.Y. and Li,P. (2016) Structural basis for concerted recruitment and activation of IRF-3 by innate immune adaptor proteins. *Proc. Natl. Acad. Sci. U.S.A.*, **113**, E3403–E3412.
38. Fujita,I., Tanaka,M. and Kanoh,J. (2012) Identification of the functional domains of the telomere protein Rap1 in *Schizosaccharomyces pombe*. *PLoS One*, **7**, e49151.
39. Yamazaki,H., Tarumoto,Y. and Ishikawa,F. (2012) Tel1(ATM) and Rad3(ATR) phosphorylate the telomere protein Ccq1 to recruit telomerase and elongate telomeres in fission yeast. *Genes Dev.*, **26**, 241–246.